EFFECT OF NITROGEN AND BORON ON THE DEVELOPMENT OF ACICULAR FERRITE IN REHEATED C-Mn-Ti STEEL WELD METALS

M.N. Ilman, R.C. Cochrane and G.M. Evans

ABSTRACT

The transformation behaviour of C-Mn-Ti alloyed steel weld metals with different levels of nitrogen and boron contents has been investigated using a dilatometric technique in combination with transmission electron microscopy (TEM) associated with microanalysis techniques, i.e. energy dispersive X-ray analysis (EDXA) and electron energy loss spectroscopy (EELS) in order to clarify the role of nitrogen and boron on the nucleation and growth processes of weld metal microstructure in particular acicular ferrite which gives high strength and improved impact toughness of steel weld metals.

Results of this investigation showed that the addition of a small amount of boron, typically 40 ppm to a C-Mn-Ti weld metal was sufficient to significantly reduce the transformation start temperature with a decrease in the amount of grain boundary ferrite and a concommittant rise in the amount of acicular ferrite. Further decrease in the transformation start temperature was observed as the level of boron content was increased up to approximately 160 ppm resulting in the formation of bainitic microstructures. However, a subsequent addition of nitrogen around 240 ppm to this type of weld metal increased the transformation temperature and modified the weld microstructure marked by the presence of intragranular acicular ferrite and polygonal ferrite which nucleated on multiphase inclusions principally of the 'TiO' type but on which has formed BN. This finding seems to suggest that BN is a potent substrate for nucleating ferrite and the amount of acicular ferrite in Ti-B-N system is controlled by the balance between BN as an energetically favourable site for acicular ferrite nucleation and soluble boron which acts as a hardenability element suppressing grain boundary ferrite formation.

IIW-Thesaurus keywords: Ferrite; Austenite; Phase transformation; Inclusion.

1 Introduction

The use of B containing consumables for submerged arc welding of pipeline steels has been responsible for dramatic improvements in weld toughness [1-3]. Together with Ti, B raises the impact toughness of C-Mn steel weld metals by suppressing the nucleation of grain-boundary polygonal ferrite, increases the effective hardenability of the austenite and causing subsequent acicular ferrite transformation to occur intragranularly. Whilst the role of inclusions in the formation of acicular ferrite is well recognised, details of the influence of B have been lacking and until now the focus has been on identifying the types of inclusions responsible. However, it is clear that B is intrinsically linked to the formation of AF and there appear to be three major mechanisms [4-6] by which Ti and B improve weld metal toughness :

- Boron tends to react with nitrogen hence reducing free nitrogen from solution in the austenite whereas titanium protects the boron from oxidation.
- Soluble boron easily segregates at prior austenite grain boundaries and retards the nucleation of grain boundary (allotriomorphic) ferrite ferrite during austenite to ferrite transformation.
- The presence of TiO inclusions promotes intragranular nucleation of acicular ferrite.

Consequently, increasing nitrogen should have a strongly detrimental effect on Ti-B type weld metals [7] since the formation of BN is more likely. However, from recent studies, it has become increasingly evident that nitrogen can also be beneficial when it is added properly to Ti-B containing weld metals. Lau ***et al.*** [5] reported that the critical balance between Ti, B, N and O affected microstructure and toughness of weld metal and they claimed that the optimum toughness of Ti-B containing weld metals was achieved when the amount of nitrogen in the weld metals was around 70 ppm. More recently, Evans [8] has suggested that nitrogen affects the microstructure and mechanical properties of Ti-B type weld metals in a complex manner depending on Ti and B contents. According to Evans, the toughness of weld metals containing an excess of boron, typically 160 ppm, can be improved by a proper addition of nitrogen which would have been thought impossible previously. However, the exact mechanism of how these alloying elements in particular Ti, B, N and O to affect microstructure and transformation behaviour is still not yet clearly understood. Therefore, the present investigation attempts to clarify the role of N on the transformation behaviour of Ti-B type weld metals

Doc. IIW-2265, recommended for publication by Commission II "Arc Welding and Filler Metals."

in particular acicular ferrite formation. Unfortunately, it is not possible to measure transformation kinetics directly during the welding process so that the most appropriate method used in the present investigation is to simulate weld metal transformation dilatometrically using samples taken from as deposited weld metals. Results obtained in this way would apply, therefore, particularly well to the coarse grain reheated regions of a multipass weld.

2 Experimental procedures

2.1 Materials

The MMA samples were prepared by Oerlikon Welding Limited, Zurich, Switzerland according to ISO 2560-1973. Details of sample preparation are given elsewhere [9]. Weld metal specimens with different levels of B and N were deposited with their chemical compositions are given in Table 1.

2.2 Dilatometry

Dilatometric technique was used to study the $\gamma \rightarrow \alpha$ phase transformation of Ti-B-N weld metals during continuous cooling. Specimens were machined in the form of hollow cylinder with standard specimen dimensions, i.e. 10 mm long by 5 mm outside diameter with a wall thickness of 1 mm. The axis of each specimen was parallel to the weld direction. The specimens were subjected to controlled thermal cycle which consisted of austenitization at 1250 °C for 2 minutes followed by continuous cooling at a typical weld cooling rate of 13 °C/s from 800 to 500 °C.

2.3 Interrupted quench experiments

The nucleation and growth processes during development of the weld metal microstructure were studied using interrupted quench experiments. Specimens were machined in the form of solid cylinder with the diameter of 3 mm and 5 mm in length. A K-type thermocouple was welded at a traverse section of each solid cylinder specimen using a spot welder to monitor temperature during thermal cycle. Specimens were heated in a furnace for 2 minutes at 1250 °C to reach austenite phase field. Subsequently, the specimens were withdrawn from the furnace to cool in the atmosphere while the temperature was monitored by means of thermocouple attached to the specimens. On reaching temperatures in the range 650 and 720 °C, but typically 700 and 680 °C, the specimens were quenched into water to obtain partially transformed microstructure.

2.4 Metallography

Microstructural examinations were carried out on transverse sections of the weld metals using standard metallographic technique including mounting, grinding, polishing and etching in 2% nital.

Microanalysis of inclusions was carried out using a PHILIPS CM20 transmission electron microscope equipped with energy dispersive X-ray (EDX) spectrometer. Electron energy loss spectroscopy (EELS) was also used to identify light elements such as B and N. Specimens were in the forms of both thin foils and carbon extraction replicas supported on copper grids.

3 Results and discussion

Figure 1 shows microstructural changes due to different levels of B and N contents. It can be seen that in a low level of N, a C-Mn steel weld metal X containing 400 ppm Ti consists mainly of acicular ferrite and a considerable amount of grain boundary ferrite. This acicular ferrite is found to nucleate on TiO inclusions as previously reported by Mori *et al.* [10]. A small addition of B, approximately 40 ppm, reduces grain boundary ferrite giving more acicular ferrite as seen in weld metal Y. However, further addition of B up to approximately 160 ppm produces microstructure mainly bainite (weld metal U). This finding is consistent with the work of Lee *et al.* [11] which showed that the volume fraction of acicular ferrite decreased with increasing boron content from 32 ppm to 103 ppm. Nitrogen additions to the B-free, weld metal X, does not significantly changes the microstructure as seen in weld metal X2 whereas in the weld metal Y with 40 ppm B, the effect of N starts to emerge marked by the presence of coarse grain boundary ferrite as shown in weld metal Y2. It seems likely that the effect of soluble B which

Table 1 – Chemical composition of Ti-B-N steel weld metals

WELD		C	Mn	Si	S	P	Ti	B	N	O
		wt%					ppm			
Low N	X	0.069	1.47	0.45	0.005	0.006	410	2	77	282
	Y	0.070	1.57	0.45	0.006	0.010	390	39	83	308
	U	0.073	1.52	0.40	0.006	0.011	390	158	84	290
High N	X2	0.068	1.46	0.47	0.007	0.006	450	2	249	297
	Y2	0.069	1.51	0.36	0.007	0.008	410	44	232	292
	U2	0.066	1.40	0.36	0.007	0.012	390	167	217	297

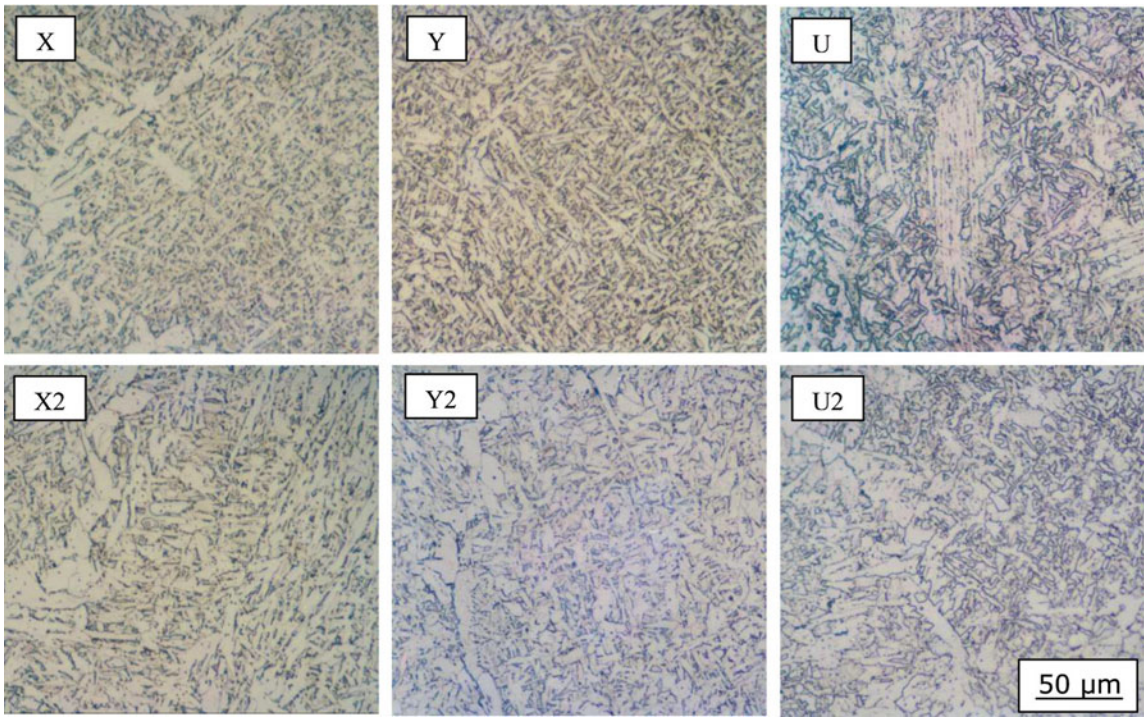

Figure 1 — Photomicrographs of as deposited Ti-B-N type weld metals

inhibits grain boundary ferrite is blocked by soluble N. A noticeable change due to N addition is observed in a high B containing weld metal U in which bainitic structure is replaced by intragranular polygonal and acicular ferrite as seen in weld metal U2.

Dilatometric results of Ti-B-N type weld metals continuously cooled at 13 °C/s are shown in Figure 2. The transformation start is associated with the formation of grain boundary ferrite (T_s), whereas the 50% transformation, (T_{50}) and peak rate transformation (T_p) temperatures is used as indicators of the comparative rates of transformation. Details are also shown in Figure 3.

Referring to Figure 2 and Figure 3, it can be seen that transformation start temperature of weld X is around 760 °C. The addition of 40 ppm B retards the start of transformation associated with the formation of grain boundary ferrite and is marked by a sharp drop in the transformation start temperature from 760 to 705 °C. This result is in agreement with Babu *et al.* [12] who showed that small levels of boron, typically 20 to 40 ppm in steel resistance-seam welds retarded the austenite to ferrite transformation. As is observed in weld metal U, a further increase of B to around 160 ppm tends to decrease the transformation start temperature only slightly further. The addition of N to the weld metals with low B content do not

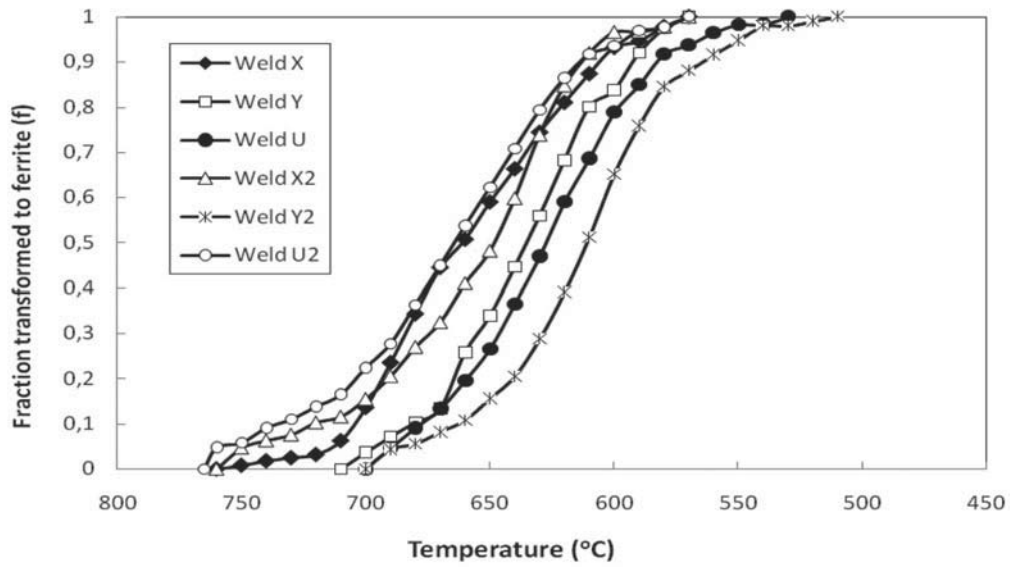

Figure 2 — Transformation kinetics of Ti-B-N type weld metals

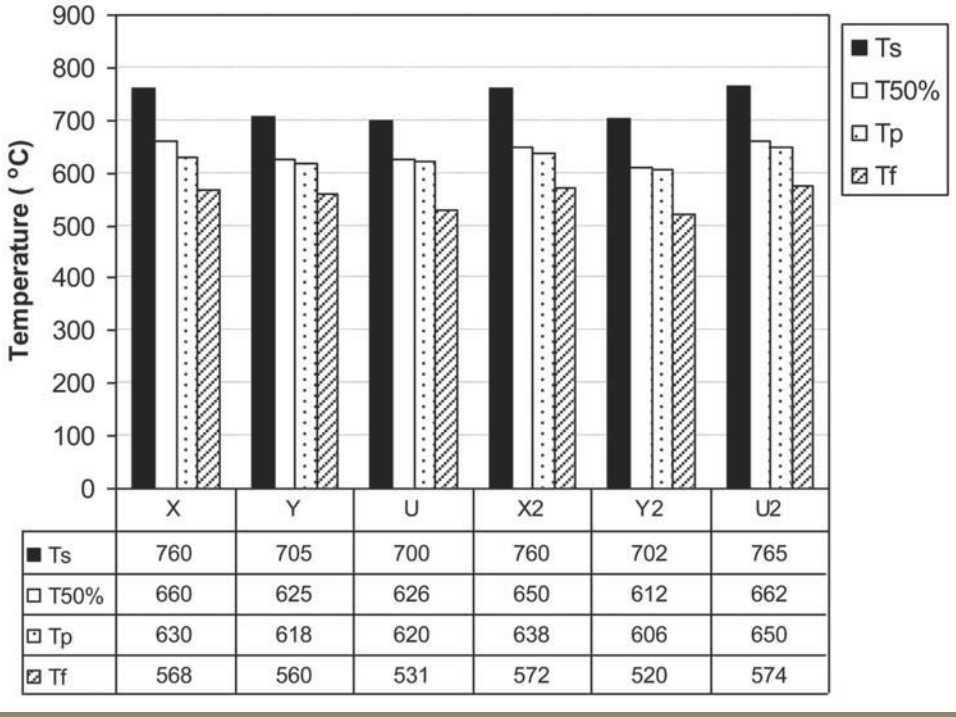

	X	Y	U	X2	Y2	U2
Ts	760	705	700	760	702	765
T50%	660	625	626	650	612	662
Tp	630	618	620	638	606	650
Tf	568	560	531	572	520	574

Figure 3 – Transformation temperatures of Ti-B-N type weld metals

significantly affect transformation temperatures as seen in X2 and Y2 but in the case of the weld with a high level of B (weld U), a sharp increase in the transformation start temperature is observed when 240 ppm N is added. Note, however, that the peak rate of transformation is lowest in weld Y2 corresponding with the larger amount of acicular ferrite. Conversely, the high peak transformation rates are found in weld U2 which has the largest amount of grain boundary polygonal ferrite. All microstructures found in the reheated welds after dilatometry are consistent with the microstructures present in the Ti-B-N welds except, obviously, that the austenite grain size structure was more equiaxed.

As the early stages of the austenite to ferrite transformation in the reheated Ti-B-N welds appear to be more strongly affected by composition, this phase of transformation was studied more closely using interrupted quench experiments. The resulting microstructures are shown in Figure 4. It is seen that in the absence of B, weld metal X, there is a continuous grain boundary ferrite network delineating prior austenite grain boundaries In weld Y, 40 ppm B, the growth of ferrite along austenite boundaries is reduced and is significantly less than that of weld X. A further increase in B, weld U, suppresses grain boundary ferrite even more leading to a change in the morphology of grain boundary ferrite to discrete globular particles located at austenite triple grain boundary intersections. However, the effect of increasing N, therefore reducing soluble B, is to greatly increase the amount of grain boundary ferrite, weld U2.

The mechanism in which soluble B segregates at prior austenite grain boundaries and lowers their energy thereby retarding the nucleation of grain boundary ferrite is still matter of controversy. However, if this mechanism is operative then the classical theory of nucleation and growth may explain the morphology of grain boundary ferrite due to B addition. Figure 5 shows nucleation of a new solid phase (α) at austenite (γ) grain boundaries. The free energy associated with the embryo (ΔG), [13-15], is given by

$$\Delta G = -V\Delta G_V + A_{\alpha\gamma}\,\gamma_{\alpha\gamma} - A_{\gamma\gamma}\,\gamma_{\gamma\gamma} \qquad (1)$$

where ΔG_v is the chemical volume free energy of the embryo of a new phase (α), V is volume of the embryo, $A_{\alpha\gamma}$ is the area of α/γ interface of energy $\gamma_{\alpha\gamma}$ created and $A_{\gamma\gamma}$ is the area of γ/γ grain boundary of energy $\gamma_{\alpha\alpha}$ destroyed during the process. The optimum shape of nucleus is achieved if it forms a spherical cap to minimize the total interfacial free energy [13] with θ is given by :

$$\cos\theta = \gamma_{\gamma\gamma} / 2\gamma_{\alpha\gamma} \qquad (2)$$

According to Eq.(1), a reduction in grain boundary energy ($A_{\gamma\gamma}\gamma_{\gamma\gamma}$) due to boron segregation increases the energy barrier to nucleation hence retarding grain boundary ferrite. In addition, the surface free energy ratio ($\cos\theta$) is low so that the dihedral angle between the interphase boundaries, θ , is large. As a result, the growth of grain boundary ferrite is in the form of discrete globular particles or more equiaxed morphologies at and along prior austenite boundaries. In the absence of B, the reduction of grain boundary energy due to segregation is nil therefore, the dihedral angle is low, typically less than 60° so that grain boundary ferrite is expected to form a continuous network along the austenite grains.

The changes in the austenite to ferrite phase transformation in reheated Ti-B-N steel weld metals may also be

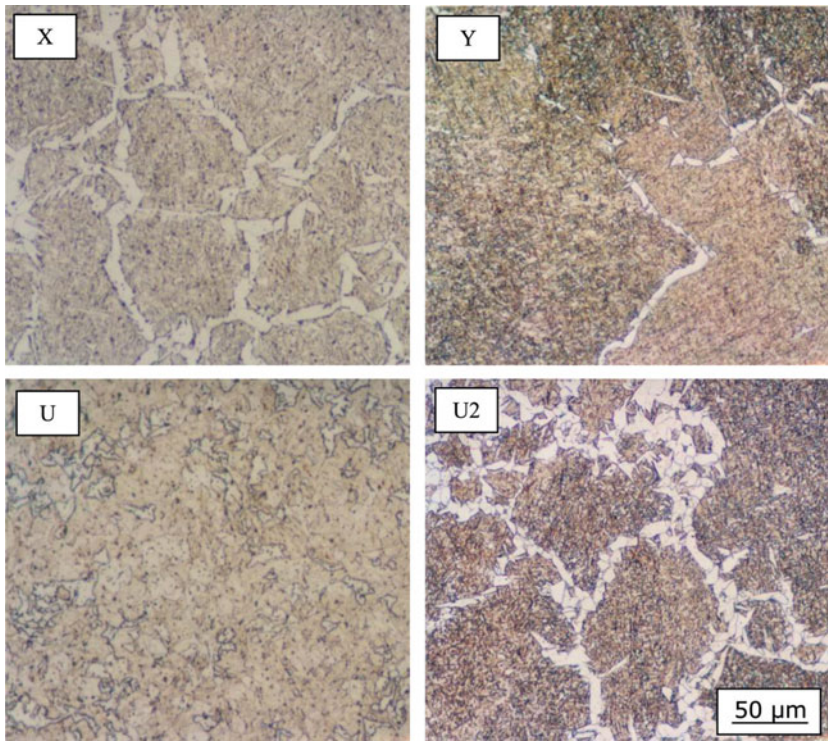

Figure 4 – Partially transformed microstructures of Ti-B-N weld metals quenched at 700 °C except weld metal U (680 °C) during continuous cooling

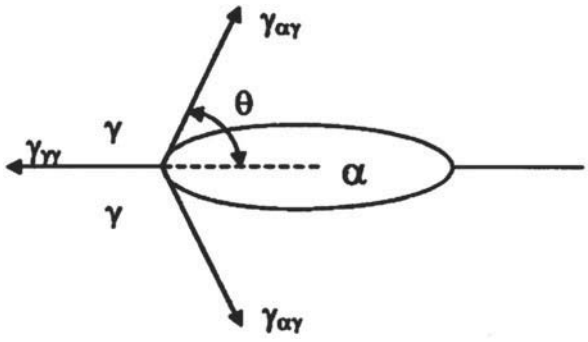

Figure 5 – Nucleation of ferrite along austenite grain boundaries

related to the nature of inclusions. Microanalysis results, as in Figure 6 b), of inclusions present in the C-Mn-Ti alloyed steel weld metals show that inclusions, largely monophase, consist principally of Ti with a small amount of Mn together with O. Elements such as S and Cu are often identified in the inclusions probably in the form of MnS and/or CuS. In general, the inclusions under study appear to be homogeneous with no distinct phase boundaries. From thermodynamic analysis, Ti can form various oxides such as TiO, Ti_2O_3, Ti_3O_5 and TiO_2. Of these oxides, TiO is the most stable oxide since it has the lowest Gibbs free energy (ΔG) therefore TiO is the most likely to form. The present investigation seems to confirm that TiO-inclusions are effective sites for nucleation of acicular ferrite [9, 16-20].

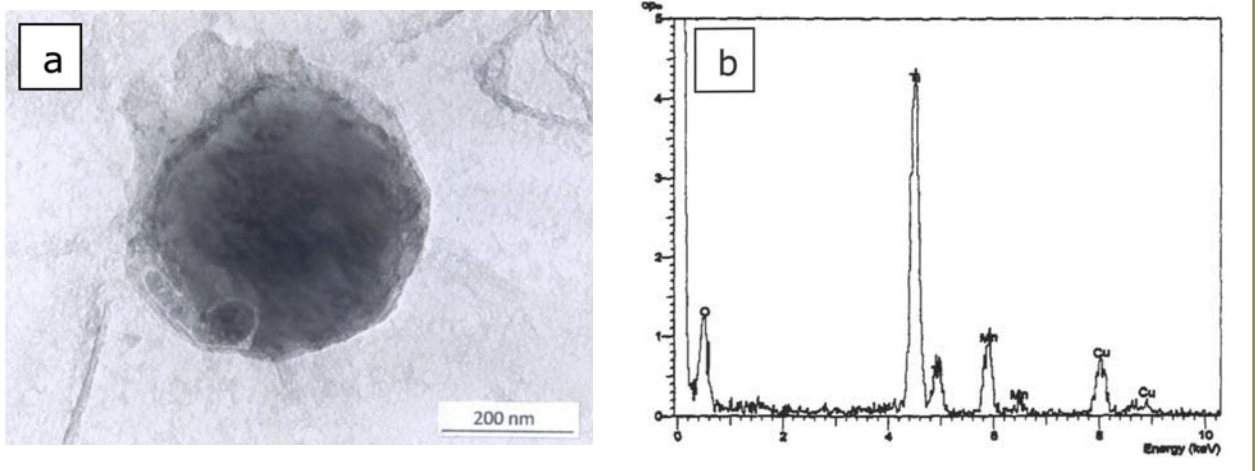

Figure 6 – An example of inclusions in C-Mn-Ti alloyed steel weld metals

Figure 7 shows a typical inclusion found in the C-Mn-Ti weld metals with high levels of both B and N contents (weld U2). It can be seen that this type of inclusions is characterized by several phases within a single inclusion. The EDX spectra taken from the core of the inclusion marked A in Figure 7 a) show the presence of mainly Ti and O with a small amount of Mn [Figure 7 b)] whereas region marked B shows the traces of Cu, Si and Mn as seen in Figure 7 c). However, result of EELS analysis in the region B shows the presence of B and N as shown in Figure 7 d). Analysis of diffraction pattern [Figure 7 e)] shows that this B-N rich phase exhibits ring patterns

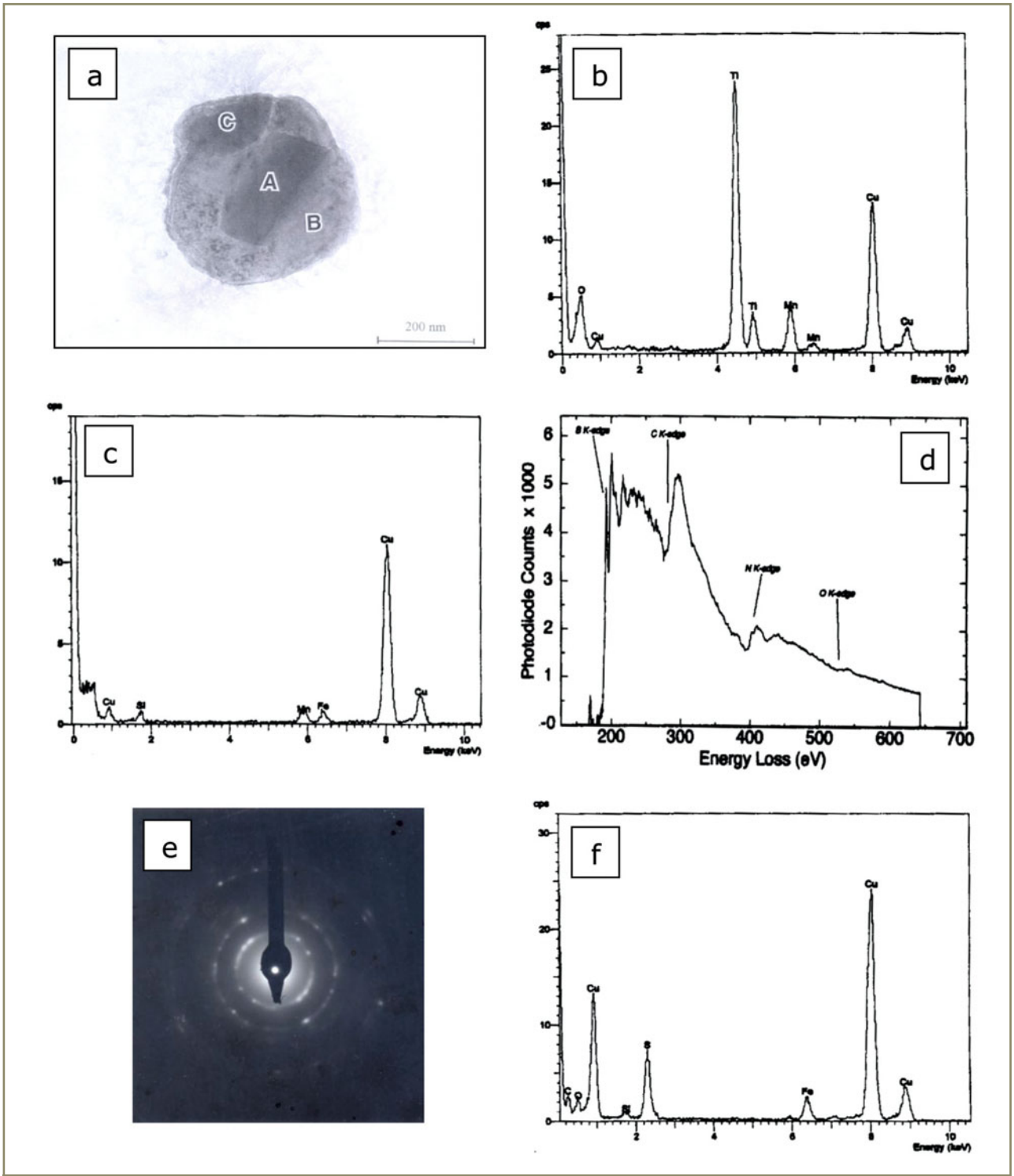

Figure 7 –
a) An example of inclusions in C-Mn-Ti alloyed steel weld metals with high B and N contents (carbon extraction replicas);
b) EDX-spectra taken from region A in Figure 7a);
c) EDX-spectra taken from region B in Figure 7 a);
d) EELS spectra taken from region B in Figure 7 a) showing the presence of B and N;
e) SADP taken from region B in Figure 7 a) showing ring pattern;
f) EDX-spectra of region C in Figure 7 a) showing Cu,S-rich phases.

belonging to BN phase. This is consistent with the observations of a number of authors [21,22] who show that BN has Debye-Scherrer ring patterns characteristic of a polycrystalline structure. The EDX-spectra obtained in region marked C shows Cu-S rich phase, probably in the form of CuS. Of note is that, this investigation was carried out using carbon replicas supported on copper grids so that peaks of K_α and K_β belong to copper which were always observed in spectra came from the cooper grids but L_α of Cu-peak which was occasionally observed may belong to copper-rich phase present in inclusions.

TEM characterizations of acicular ferrite using thin foils are shown in Figure 8 a)-d). It can be seen that acicular ferrite

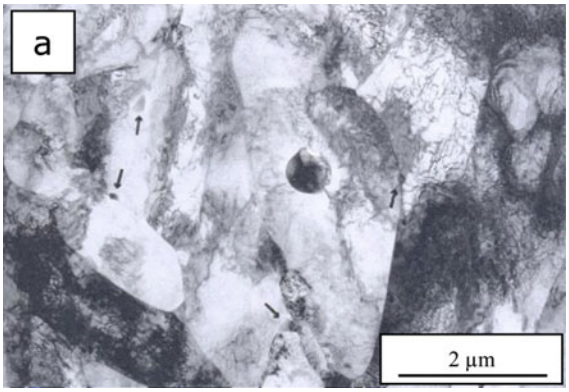

a) Acicular ferrite in weld metal U2

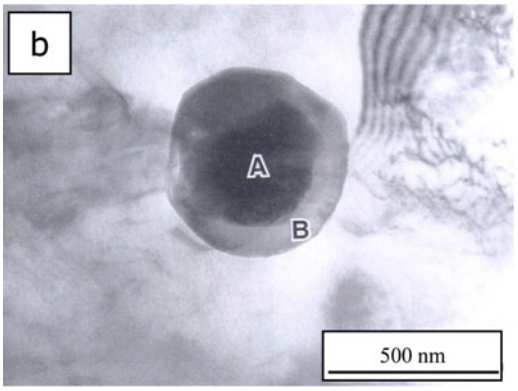

b) An example of inclusion in weld U2

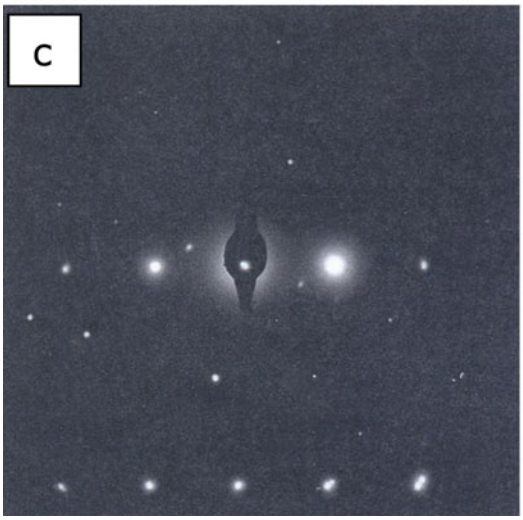

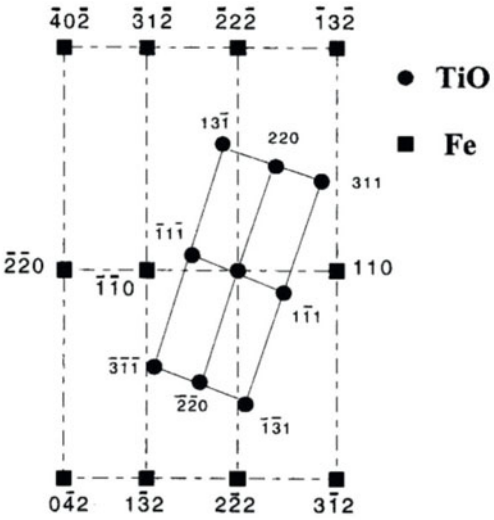

c) SADP taken from Ti-rich region marked A in Figure 8 b)

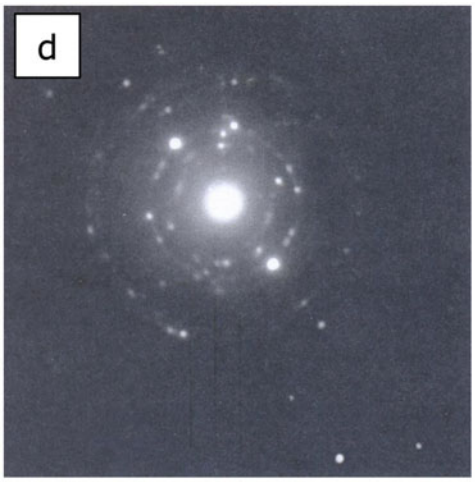

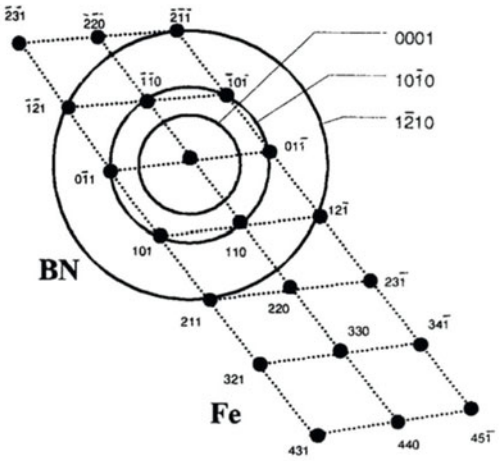

d) SADP taken from B-N rich region marked B in Figure 8 b)

Figure 8 – Characterization of inclusions in the weld with high B and N contents

plates are marked by high dislocation density [Figure 8 a)] which nucleate on Ti-O rich core [region A in Figure 8 b)] surrounded by spherical shell of BN phase (region B). Selected area diffraction patterns taken from this Ti-rich region reveal this phase to be FCC with a lattice parameter of 0.412 nm as shown Figure 8 c) consistent with that of TiO ($a_o = 0.418$ nm). Again, the B-N rich phase of region B shows ring patterns [Figure 8 d)] consistent with BN where $(10\bar{1}0)_{BN}$ is closely matched with {110} planes of ferrite (α).

Another microstructural feature observed as a result of transformation in C-Mn-Ti with high B content is the presence of boron constituents as indicated by arrows in Figure 8 a) and details of these constituents are shown in Figures 9 a)- b). These constituents are found to nucleate along ferrite grains. Selected area diffraction pattern in Figure 9 c) shows that these constituents have fcc crystal structure with a lattice parameter (a_o) of 1.06 nm approximately three times larger than that of ferrite. This lattice parameter is consistent with that of iron borocarbide $Fe_{23}(BC)_6$. Of note is that the formation of iron borocarbide $Fe_{23}(BC)_6$ in steels has been extensively investigated but rarely reported in steel weld metals since the amount of B in weld metals are commonly maintained low. In steels, $Fe_{23}(BC)_6$ has been reported to form at temperature in the range of 650 to 900 °C and it reduces hardenability due to a reduction in soluble B [22-28].

The mechanism of BN formation can be assessed from the results of interrupted quench experiments as shown in Figure 10. At a temperature of 1250 °C, a large amount of BN is dissolved in austenite as indicated by the absence of BN on the TiO inclusions, Figure 10 a). This is in agreement with the solubility data for BN proposed by Fountain and Chipman [29] as follows :

$$\log k = \log [B][N] = -13970/T + 5.24 \quad (3)$$

where k is solubility product, [B] and [N] are percentages of B and N respectively given in wt%, and T is absolute temperature (K).

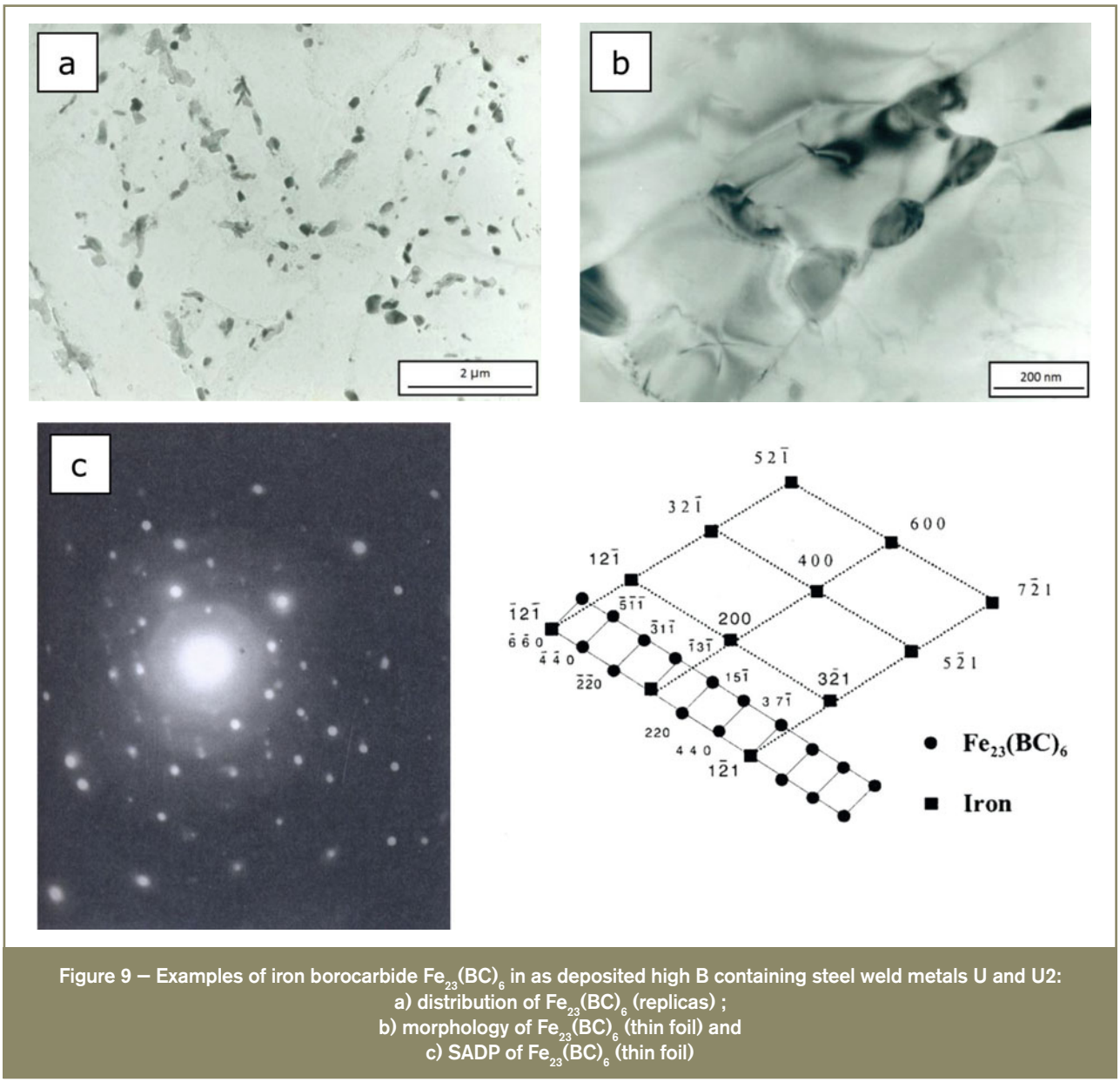

Figure 9 – Examples of iron borocarbide $Fe_{23}(BC)_6$ in as deposited high B containing steel weld metals U and U2: a) distribution of $Fe_{23}(BC)_6$ (replicas) ; b) morphology of $Fe_{23}(BC)_6$ (thin foil) and c) SADP of $Fe_{23}(BC)_6$ (thin foil)

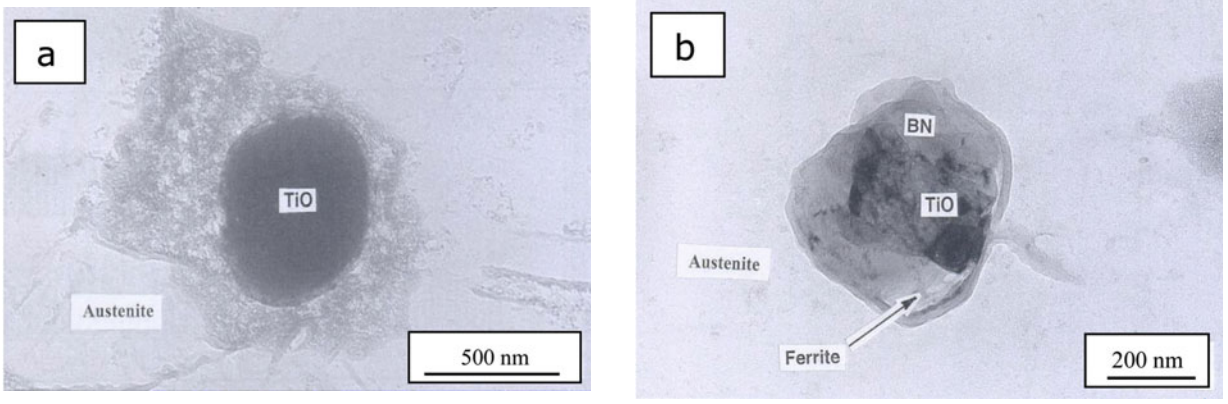

Figure 10 – (a) A TiO inclusion quenched at 1250 °C, (b) Reprecipitation of BN on TiO inclusion at 700 °C

Based on thermodynamic data it can be predicted that in Ti-B-N-O system, Ti prefers to form TiO rather than TiN and B tends to react with N to form BN not B_2O_3 [5,30]. If this assumption is operative then the temperature at which BN starts to precipitate in weld metal U2 with [B] = 0.0167 wt% and [N] = 0.0217 wt% can be calculated by substituting these values into Eq.(3), resulting in T = 1609 K (1336 °C). Similarly, for weld metal U which contains [B] = 0.0158 wt% and [N] = 0.0084 wt%, the value of T is around 1532 K (1259 °C). This suggests that precipitation of BN takes place mainly at austenite phase field during cooling. At a temperature of 700 °C as shown in Figure 10 b), a significant amount of BN has re-precipitated on a TiO inclusion and at the same time, a tiny ferrite plate is observed nucleating from this inclusion.

4 Conclusions

The basic conclusions that can be drawn from this investigation are as follows :

- The addition of B tends to retard ferrite reaction but this effect is obviated by N
- BN prefers to nucleate on TiO type inclusions and it can act as effective site for ferrite nucleation
- Microstructure in high B containing weld metals can be optimized depending on the interactions between BN, free B and $Fe_{23}(BC)_6$.

References

[1] Garland J.G. and Kirkwood P.R.: Towards improved submerged-arc weld metal, Metal Construction, 7(5), 1975, pp. 275 and (6), pp.320.

[2] Levine E. and Hill D.C.: Toughness in HSLA steel weldments, Metal Construction, 9(8), 1977, pp. 346.

[3] Evans G.M. and Baley N.: Metallurgy of basic weld metal, Abington Publishing and William Andrew Inc., England, 1977, pp. 306.

[4] Croft N.H. and Hipley R.L.: Microstructure and properties of heat treated weldments, Int. Conf.: The effects of residual, impurity and microalloying elements on weldability and weld properties, Paper 26, London, 1983.

[5] Lau T.W, Sadowski M.M., North T.H., and Weatherly G.C.: Effect of nitrogen on properties of submerged arc weld metal, Material Science and Technology, (4), 1988, pp. 53-61.

[6] Yamada T., Terasaki H. and Komizo Y.: Relation between inclusion surface and acicular ferrite in low carbon low alloy steel weld, ISIJ International, vol.49, 2009, No. 7, pp. 1059-1062.

[7] Koshio K., Ootawa M., Tonigaki T., Takino Y., Horii Y., Tsynetomi E. and Imai K.: Development of the high titanium boron bearing covered electrode, IIW Doc. II-955-81, 1981.

[8] Evans G.M.: Effect of nitrogen on C-Mn steel welds containing titanium and boron, Welding Journal, vol. 75, 1996, pp. 251-260s.

[9] ISO 2560-1973: Covered electrodes for manual arc welding of mild and low alloy steel-Code of symbols for identification.

[10] Mori N., Homma H., Okia S. and Asano K.: The behaviour of B and N in notch toughness improvement in Ti-B weld metals, IIW/ISS-IX-1158-80.

[11] Lee H.W., Kim Y.H., Lee S.H., Lee S.K., Lee K.H., Park J.U. and Sung J.H.: Effect of boron contents on weldability in high strength steel, Journal of Mechanical Science and Technology, 21, 2007, pp. 771-777.

[12] Babu S.S., Goodwin G.M., Rohde R.J. and Sielen B.: Effect of boron the microstructure of low carbon steel resistance-seam welds, Welding Journal, 77, 1998, pp. 249-253.

[13] Porter D.A. and Easterling K.E.: Phase transformations in metals and alloys, Chapman and Hall, London, 1992.

[14] Reed-Hill R.E., and Abbaschian R.: Physical Metallurgy Principles, PWS Publishing Company, 3rd ed, Boston, USA, 1995.

[15] Verhoeven J.D.: Fundamentals of Physical Metallurgy, John Willey & Sons, New York, 1975

[16] Thewlis G.: Transformation kinetics of ferrous weld metal, Materials Science and Technology, 10, 1994, pp. 110-125.

[17] Oldland R.B.: The influence of aluminium and nitrogen on the microstructures and properties of single pass submerged arc welds, Australian Welding Research, 1985, 44-56.

[18] Mills A.R., Thewlis G. and Whiteman J.A.: Nature of inclusions in steel weld metals and their influence on formation of acicular ferrite, Materials Science and Technology, 3, 1987, pp. 1051-1061.

[19] Jang J. and Indeacochea J.E. J.: Inclusion effects on submerged arc weld microstructure, Journal of Materials Science, 22, 1987, pp. 689-700.

[20] Grong O.and Matlock D.K.: Microstructure development in mild and low alloy steel weld metals, International Metal Reviews, 31, 1986, pp. 27-48.

[21] Yamanaka K. and Ohmori Y.: Effect of boron on transformation of low carbon low alloy steels Transactions ISIJ, 17, 1977, pp. 93-101.

[22] Ohmori Y.: Isothermal decomposition of an Fe-C-B austenite, Transactions ISIJ, 11, 1971, pp. 339-348.

[23] Watanabe S. and Ohtani H.: Precipitation behaviour of boron in high strength steel, Transactions ISIJ, 23, 1983, pp. 38-42.

[24] Ohmori Y. and Yamanaka K.: Hardenability of boron-treated low carbon low alloy steel, in Boron in Steel, Wisconsin AIME, 1979, pp. 44-60.

[25] Maitrepierre Ph., Thivellier D. and Tricot R.: Influence of boron on the decomposition of austenite in low carbon alloyed steels, Metallurgical Transactions, 6A, 1975, pp. 287-301.

[26] Melloy G.F., Silmmon P.R. and Podgursky P.P.: Optimizing the boron effect, Metallurgical Transactions, 4, 1973, pp. 2279-2289.

[27] Matrepierre Ph., Rofes-Vernis J. and Thivellier D.: Hardenability concepts in the application to steel, AIME, 1978, pp. 421-447.

[28] Jung J.G., Kim J., Noh K.M., Park K.K. and Lee Y.K.: Effects of B on microstructure and hardenability of resistence seam welded HSLA linepipe steel, Science and Technology of Welding and Joining, 17, 2012, No. 1, pp. 77-84.

[29] Fountain R.W. and Chipman J.: Transactions AIME, 224, 1962, pp. 559.

[30] Oikawa K. and Ishida K.: Effect of titanium addition on the formation and distribution of MnS inclusions in steel during solidification, Transactions ISIJ, 37 (4), 1997, pp. 332-338.

About the authors

Dr. M.N. Ilman (ilman_noer@ugm.ac.id) is with the Department of Mechanical and Industrial Engineering, Gadjah Mada University, Indonesia. Prof. R.C. Cochrane (r.cochrane.cochrane@btinternet.com) was formerly British Steel Professor of Ferrous Metallurgy and is Visiting Professor at the University of Leeds, UK. Dr. G.M. Evans (gmevans@globalnet.co.uk) was formerly with Oerlikon Industries Gmbh and is now a consultant. The work reported was carried out at the University of Leeds, UK.